Published OnlineFirst December 13, 2010; DOI: 10.1158/1078-0432.CCR-10-2258

Cancer Therapy: Preclinical

Clinical Cancer Research

Targeting the Urokinase Plasminogen Activator Receptor Inhibits Ovarian Cancer Metastasis

Hilary A. Kenny[1], Payton Leonhardt[1], Andras Ladanyi[1], S. Diane Yamada[1], Anthony Montag[2], Hae Kyung Im[3], Sujatha Jagadeeswaran[1], David E. Shaw[4], Andrew P. Mazar[5], and Ernst Lengyel[1]

Abstract

Purpose: To understand the functional and preclinical efficacy of targeting the urokinase plasminogen activator receptor (u-PAR) in ovarian cancer.

Experimental Design: Expression of u-PAR was studied in 162 epithelial ovarian cancers, including 77 pairs of corresponding primary and metastatic tumors. The effect of an antibody against u-PAR (ATN-658) on proliferation, adhesion, invasion, apoptosis, and migration was assessed in 3 (SKOV3ip1, HeyA8, and CaOV3) ovarian cancer cell lines. The impact of the u-PAR antibody on tumor weight, number, and survival was examined in corresponding ovarian cancer xenograft models and the mechanism by which ATN-658 blocks metastasis was explored.

Results: Only 8% of all ovarian tumors were negative for u-PAR expression. Treatment of SKOV3ip1, HeyA8, and CaOV3 ovarian cancer cell lines with the u-PAR antibody inhibited cell invasion, migration, and adhesion. *In vivo*, anti-u-PAR treatment reduced the number of tumors and tumor weight in CaOV3 and SKOV3ip1 xenografts and reduced tumor weight and increased survival in HeyA8 xenografts. Immunostaining of CaOV3 xenograft tumors and ovarian cancer cell lines showed an increase in active-caspase 3 and TUNEL staining. Treatment with u-PAR antibody inhibited α_5-integrin and u-PAR colocalization on primary human omental extracellular matrix. Anti-u-PAR treatment also decreased the expression of urokinase, u-PAR, β_3-integrin, and fibroblast growth factor receptor-1 both *in vitro* and *in vivo*.

Conclusions: This study shows that an antibody against u-PAR reduces metastasis, induces apoptosis, and reduces the interaction between u-PAR and α_5-integrin. This provides a rationale for targeting the u-PAR pathway in patients with ovarian cancer and for further testing of ATN-658 in this indication. *Clin Cancer Res; 17(3); 459–71. ©2010 AACR.*

Introduction

Ovarian cancer is the 5th leading cause of cancer death among US women. It has the highest mortality rate of all gynecologic tumors because most patients will experience recurrences and develop chemoresistant disease (1). The mechanism of ovarian cancer metastasis differs from that of hematogeneously metastasizing tumors, because ovarian cancer cells disseminate from the primary site and are carried by peritoneal fluid to peritoneal surfaces within the abdominal cavity, including the omentum. The first step of metastasis to these sites involves a tightly regulated process of attachment, migration, and invasion to, and, proliferation on, mesothelium covered surfaces (2, 3).

A number of factors have been implicated as mediators of ovarian cancer metastasis, including integrins, growth factors, and proteases. The urokinase-type plasminogen activator (urokinase/uPA) is a serine protease that is first secreted as a proenzyme (pro-urokinase) and is then activated by proteolytic cleavage after binding to its specific cell surface receptor, the urokinase receptor (u-PAR; refs. 4, 5). Urokinase catalyzes the activation of plasminogen to plasmin, which is critical for remodeling of the extracellular matrix (ECM). Besides regulating and focusing proteolysis at the invading edge of a tumor, u-PAR plays a critical role in cancer progression through its interaction with integrins and vitronectin and as a regulator of angiogenesis (6).

Authors' Affiliations: Departments of [1]Obstetrics and Gynecology/Section of Gynecologic Oncology-Center for Integrative Science, [2]Pathology, and [3]Health Studies, University of Chicago, Chicago, Illinois; [4]D.E. Shaw Research and Center for Computational Biology and Bioinformatics, Columbia University, New York; and [5]Chemistry of Life Processes Institute and Robert H. Lurie Comprehensive Cancer Center, Northwestern University, Evanston, Illinois

Note: Supplementary data for this article are available at Clinical Cancer Research Online (http://clincancerres.aacrjournals.org/).

Corresponding Authors: Hilary A. Kenny or Ernst Lengyel, Department of Obstetrics and Gynecology/Section of Gynecologic Oncology, University of Chicago, 5841 South Maryland Avenue, MC 2050, Chicago, IL 60637. E-mail: hkenny@uchicago.edu or elengyel@uchicago.edu

doi: 10.1158/1078-0432.CCR-10-2258

Published OnlineFirst December 13, 2010; DOI: 10.1158/1078-0432.CCR-10-2258

Translational Relevance

The urokinase plasminogen activator receptor (u-PAR) is an interesting and promising therapeutic target because of its important role in several tumor cell functions. We demonstrate that inhibiting the u-PAR with an antibody blocks the adhesion, migration, invasion, and metastasis of different ovarian cancer cells *in vitro* and *in vivo*, while affecting u-PAR's regulation of adhesion receptors. We, therefore, believe that targeting the u-PAR system may enable us to block key steps of ovarian cancer progression and provide an approach appropriate for clinical evaluation.

The expression of the uPA/u-PAR proteolytic system has been demonstrated in a number of different cancer types, and high-endogenous intratumoral levels of both uPA and u-PAR are often present in advanced metastatic disease (7). In patients with ovarian cancer, high levels of uPA, soluble u-PAR, and/or u-PAR have been detected in serum, ascites, and ovarian cancer tumors (primary and metastatic; summarized in Supplementary Table S1). However, it is not clear whether u-PAR is also a prognostic marker in patients with ovarian cancer or what percentage of epithelial ovarian carcinomas actually express u-PAR. Moreover, the specific role of u-PAR in regulating the adhesion, migration, invasion, and metastasis of epithelial ovarian cancer, which are the key steps in ovarian cancer metastasis, remains to be determined.

Several approaches have been tested that target the u-PAR in preclinical models. Small molecules and peptides have been used to block the interaction of urokinase with the u-PAR, affecting downstream signaling. An antisense approach showed that the invasiveness of tumor cells was directly proportional to the density of surface u-PAR expression on cancer cells (8). Gondi and colleagues used a small hairpin RNA to target u-PAR and showed a 65% regression of established gliomas in an intracranial tumor model (9). These and other studies clearly show that the u-PAR is a potential target for cancer treatment. In view of the multifunctional properties of the u-PAR in the biology of epithelial tumors, and given that antibody-based therapies have been established as clinically feasible and efficacious, we decided to test the antitumor effects of an antibody against u-PAR in several ovarian cancer models. Our goal was to determine if u-PAR inhibition is a viable strategy that should be further developed for ovarian cancer treatment.

We show here that the u-PAR is widely expressed in primary and metastatic ovarian carcinomas and that u-PAR inhibition, using a monoclonal antibody (ATN-658), reduces ovarian tumor metastasis in several preclinical models through the induction of apoptosis and the inhibition of u-PAR interactions with integrins and the ECM.

Materials and Methods

Reagents and cell lines

Mouse monoclonal antibodies (IgG_1) against u-PAR (ATN-658 for treatment and ATN-615 for immunohistochemistry) were developed and provided by Attenuon, LLC. Both antibodies were raised against the D2D3 fragment of u-PAR immunized into Balb/C mice and bound to different epitopes as previously described (10). The CaOV-3 human ovarian cancer cell line was from ATCC (American Type Culture Collection). SKOV3ip1 and HeyA8 cells were provided by Dr. Gordon Mills. Cell lines were validated by short tandem repeat (STR) DNA 'fingerprinting using the AmpF(θ)STR Identifiler PCR amplification kit (Applied Biosystems). The STR profiles were compared with known ATCC fingerprints, to the Cell Line Integrated Molecular Authentication database, and to the MD Anderson fingerprint database. MONTY-1 was established by us (11). The α_5-integrin antibody used for immunofluorescence was purchased from Santa Cruz Biotechnology . The $\alpha_v\beta_3$-integrin antibody (LM 609), β_3-integrin antibody (B3A), and α_5-integrin antibody (P1D6) were from Chemicon. Antibodies used in immunoblots for uPA (UK-1) was purchased from American Diagnostics Inc., and for u-PAR, a rabbit polyclonal antibody, was provided by Attenuon, LLC. Antibodies against FGFR1 (#3472), caspase-3 (5A1E), and cleaved caspase-3 (3G2) were from Cell Signaling. The rabbit urokinase antibody was from Abcam. Quantitative real-time PCR primers for uPA, u-PAR, FGFR1, β_3-integrin, and α_5-integrin were purchased from Applied Biosystems.

Patient tissue samples

Tissue blocks from 162 patients with International Federation of Gynecology and Obstetrics (FIGO) stage I–IV ovarian cancer, who had undergone surgery performed by a gynecologic oncologist at the University of Chicago, were selected by a gynecologic pathologist (A.M.) after obtaining Institutional Review Board (IRB) approval. Clinical and histopathologic informations were collected and updated regularly as previously reported (12).

Tissue microarray and immunohistochemistry

Tissue microarray slides were deparaffinized and incubated with anti-u-PAR (mouse ATN-615) at a 1:200 dilution. The slides were stained using the Envision avidin–biotin-free detection system and counterstained with hematoxylin. Immunoscoring was performed with the Automated Cellular Imaging System (ACIS) (12). Within the tissue core, the most representative tumor area of standardized size was selected at 100× magnification and the fraction of positively stained cells and the intensity of the staining read with the ACIS and confirmed by a gynecologic pathologist (A.M.). Readings were reported as a low (ACIS score < 120) or high (ACIS score ≥ 120) level of u-PAR expression in tumors. The median level of u-PAR was an ACIS score of 131. Overall survival estimates were

Published OnlineFirst December 13, 2010; DOI: 10.1158/1078-0432.CCR-10-2258

computed using the Kaplan–Meier method, and comparisons between groups were analyzed using the log-rank test. Differences between primary tumors and corresponding metastases were evaluated using a 2-sample *t* test with pooled variance.

Immunoblot analysis

Cells were lysed in RIPA buffer and immunoblot analysis performed as previously described (12). The following dilutions of antibodies were used: anti-u-PAR (rabbit polyclonal from Attenuon, LLC; 1:2,000), anti-uPA (UK-1; 1:1,000), anti-β_3-integrin (B3A; 1:2,000), and anti-FGFR1 (#3472; 1:2,000).

Three-dimensional omental culture system

Specimens of human omentum were obtained from patients undergoing surgery for benign conditions under an IRB approved by the University of Chicago. Primary human mesothelial cells and fibroblasts were isolated from the omentum and purification was verified by vimentin, keratin 8, and prolyl-hydroxylase immunohistochemistry (13, 14). The three-dimensional (3D) omental culture system was assembled by plating 2,000 human primary fibroblasts per well plus collagen; 18 hours later 10,000 human primary mesothelial cells were added to a 96-well culture plate.

Adhesion assays

Matrigel (0.5 μg) or the 3D omental culture assembled with 4,000 human primary fibroblasts and 20,000 human primary mesothelial cells was used to coat a 96-well dish, and a 4 hour adhesion assay was performed with fluorescently labeled ovarian cancer cells (13). Cells were treated with mouse IgG or anti-u-PAR (20 μg/mL) at the time of cell plating or pretreated for 18 hours. Differences between treatments were evaluated using an unpaired, 2-tailed Student's *t* test.

Migration and invasion assay

Fifty thousand cells (unlabeled for collagen type I or Matrigel and fluorescently labeled for 3D omentum culture) were plated on each well of a 24-well transwell plate that was either precoated with 20 μg of collagen I, Matrigel, or contained the 3D omental culture system. The migration and invasion assays were performed as previously described (13). Differences between treatments were evaluated using an unpaired, 2-tailed Student's *t* test.

Omental ECM isolation

ECM was isolated from primary human omentum, the most common site of ovarian cancer metastasis, in order to provide an environment that is more comparable to the endogenous situation. This omental ECM was used to determine the localization of u-PAR on ovarian cancer cells. Fresh omentum was cut into small sections (1 to 2 mm in thickness) and suspended in dispase solution (Sigma–Aldrich) at 2 mg/g of tissue and incubated for 2 hours at 4°C to remove all cells from the ECM. The tissue sections were rubbed over a cell sieve to separate the intact cells from the remaining ECM. Matrices were homogenized in high salt buffer [0.05 mol/L Tris (pH 7.4), 3.4 mol/L NaCl, 4 μmol/L *N*-ethylmaleimide] containing protease inhibitors (0.001 mg/mL pepstatin, 0.01 mg/mL aprotonin, 2 mmol/L orthovanadate, and 1 mmol/L PMSF) and centrifuged 3 times at 7,000 g for 15 minutes. Supernatant was discarded. The pellet was incubated in 2 mol/L urea buffer [0.15 mol/L NaCl and 0.05 Tris (pH 7.4)] at 1 mL of buffer/g of tissue rotating for 48 hours at 4°C to solubilize ECMs. The solution was centrifuged at 14,000 g for 20 minutes and supernatant containing ECM collected. The concentration and sizes of ECMs isolated were analyzed using bicinchoninic acid protein concentration assay and SDS-PAGE. The protocol was adapted from Abberton and colleagues (15).

Immunofluorescence

Cells were plated on glass coverslips coated with omental ECM and 24 hours later FITC-labeled uPA was added for 30 minutes. For colocalization experiments, the cells were fixed with 4% paraformaldehyde in PBS for 30 minutes and immunofluorescence was performed. Primary antibodies against active caspase-3 (1:200) or α_5-integrin (1:300) and secondary antibodies goat anti-mouse or anti-rabbit Alexafluor 645 (1:200; Invitrogen) were used. Nuclear counterstain was performed with Hoechst. Imaging was performed using a Zeiss LSM510 confocal microscope. For all 3D and colocalization experiments, Imaris 3D visualization and analysis software (Bitplane Inc.) was used. The ImarisColoc and Measurement Pro applications were used to measure mean percent colocalization of fluorescein isothiocyanate (FITC)-labeled uPA and α_5-integrin in cells from the confocal images obtained with a 488 and 645 lasers on the Zeiss LSM510. Both automated (reported) and manually set thresholds were used in the analysis, but there was no difference in the 2 analyses. An independent sample *t* test was used to determine significance of the mean percent of FITC-labeled uPA and α_5-integrin colocalization in control and anti-u-PAR-treated SKOV3ip1 cells.

Animal experiments

CaOV3 (2×10^6), HeyA8 (1×10^6), or SKOV3ip1 (1×10^6) cells were injected intraperitoneally (i.p.). IgG or anti-u-PAR (ATN-658) (10 mg/kg) was administered twice a week starting on day 7 post tumor cell injection. Paclitaxel (0.03 mg/mouse) was injected once a week for 3 weeks (13 mice/group for CaOV3 cells, 10 mice/group for SKOV3ip1 or HeyA8 cells) starting on day 10. The 1.5 mg/kg dose was used to achieve an approximately 50% inhibition in metastasis to allow the evaluation of any additive or

Published OnlineFirst December 13, 2010; DOI: 10.1158/1078-0432.CCR-10-2258

synergistic effect of the u-PAR antibody. The mice were sacrificed 63 (CaOV3), 22 (HeyA8), or 28 (SKOV3ip1) days after cancer cell injection, and the number of tumor colonies counted, dissected, collected, and weighed as described previously (12) and analyzed by unpaired, 2-tailed Student's *t* test. For the survival study, HeyA8 cells (1×10^6) were injected i.p. into female athymic nude mice (10 mice/group), and animals were sacrificed at the first signs of distress per institutional guidelines. Kaplan–Meier survival estimates were calculated to determine significant changes in the survival study. Procedures involving animal care were approved by the Committee on Animal Care at the University of Chicago.

Quantitative real-time reverse transcriptase-polymerase chain reaction

Trizol reagent was used to isolate RNA according to manufacturer instructions (Invitrogen). Real-time quantitative reverse transcriptase-polymerase chain reaction (qRT-PCR) was performed using the Prism7500 TaqMan PCR detector. Relative levels of mRNA gene expression were calculated using the $2^{-\Delta\Delta CT}$ method (16). Differences between treatments were evaluated using an unpaired, 2-tailed Student's *t* test.

Mouse xenograft tumor immunohistochemistry and TUNEL staining

Immunohistochemistry was performed on tumors as previously described (12). TUNEL staining was performed according to the manufacturer's protocol. The slides were stained with 3,3′-diaminobenzidine reagent and counterstained with hematoxylin.

Apoptosis

SKOV3ip1 cells were treated for 48 hours with 20 μg/mL u-PAR antibody or control IgG. The sub-G1 population was analyzed by fluorescently-activated cell sorting.

Microarray

RNA from each sample was labeled using the One-Cycle Eukaryotic Target Labeling assay from Affymetrix. The fragmented biotin-labeled cRNA was hybridized to Affymetrix GeneChip Human Genome U133 plus 2.0 arrays. Gene expression data were calculated from normalization of Affymetrix data files generated from the arrays. Our probe level data were normalized using the invariant-set normalization procedure. The normalized probe level data were converted to model-based gene expression indexes (MBEI, log with base 2) to be used as the values for gene expression. All microarray procedures were performed by the Functional Genomics Facility at the University of Chicago.

Results

u-PAR expression in human ovarian carcinoma

Previous studies have reported various expression levels of u-PAR in ovarian cancer (summarized in Supplementary Table S1; refs. 17–24). To clarify the percentage of patients with u-PAR positive ovarian cancers, a tissue microarray containing tumor tissue from 135 patients with advanced (FIGO stage III/IV) and 27 patients with early cancers (stage I/II) was stained for u-PAR. Only 8% (13/162) of all patients had tumors that were negative for u-PAR expression. The u-PAR was expressed in all major histologic subtypes (serous papillary, endometrioid, mucinous, and clear cell ovarian cancers; Table 1) in the epithelial tumor compartment (Fig. 1A). Weak expression was found in the stroma, but

Table 1. u-PAR expression in human ovarian cancer

		Total number (%) (*N*=162)	u-PAR expression score	
			Low (<120) (*N*=81)	High (≥120) (*N*=82)
OvCaStage				
	I	19 (11.7)	9	10
	II	8 (4.9)	4	4
	III	93 (57.5)	45	48
	IV	42 (25.9)	22	20
Histology				
	Serous-papillary	115 (71.0)	52	63
	Endometrioid	22 (13.6)	13	9
	Clear cell	15 (9.3)	9	6
	Mucinous	10 (6.2)	6	4
Grading				
	G1	13 (8.0)	8	5
	G2	39 (24.1)	16	23
	G3	110 (67.9)	56	54
Residual tumor				
	≤1 cm	95 (58.6)	49	46
	>1	66 (40.7)	31	35
	unknown	1 (0.6)	1	0
Chemotheraphy type				
	Neo-adjuvant	19 (11.7)	8	11
	Primary	133 (82.1)	68	65
	None	10 (6.2)	4	6
Chemotheraphy				
	Taxane/Platinum	140 (86.4)	70	70
	Platinum	6 (3.8)	5	1
	Other	6 (3.7)	1	5
	None	10 (6.2)	4	6

NOTE: Clinical data of patients with stage I–IV ovarian cancer (OvCa; $n = 162$). Immunoscoring was performed with the Automated Cellular Imaging System, and the u-PAR expression scores are reported as high if greater than or equal to the median score (120) or low if less than median score.

Published OnlineFirst December 13, 2010; DOI: 10.1158/1078-0432.CCR-10-2258

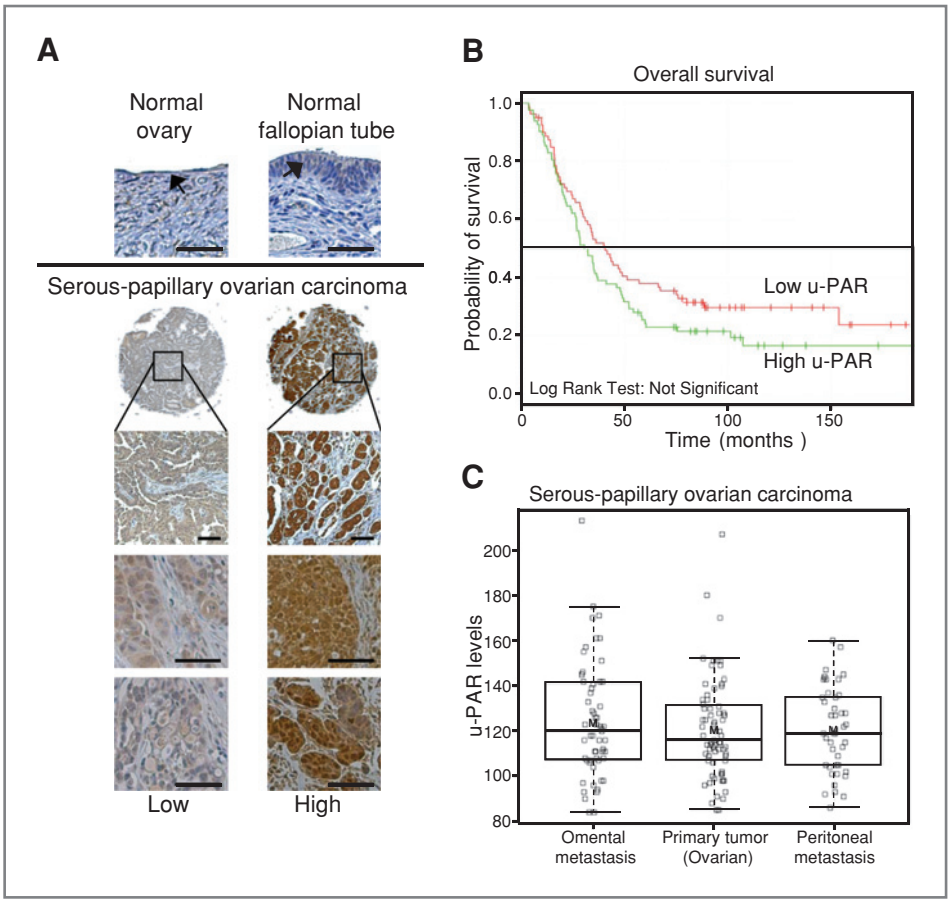

Figure 1. A, representative pictures of immunohistochemical analysis of u-PAR expression in ovary, fallopian tube, and ovarian carcinomas from 8 separate patients (4×, 100×, or 200× magnification; scale bar, 100 μm; arrow, surface epithelium). B, overall survival of patients with low or high-u-PAR expression in tumors (log rank test). C, u-PAR expression in primary and corresponding metastatic serous-papillary ovarian cancers. Immunohistochemical analysis of u-PAR expression in primary (n = 80, ovarian), omental (n = 61), and peritoneal (n = 50) tumors. Mean (thick line); 50% (box) and 95% (dotted line) of cohort.

the expression in the tumor cells was consistently stronger. In univariate analysis, expression was independent of the classic clinicopathologic parameters, including tumor grade, primary disease location (fallopian tube, peritoneum, or ovary), or ascites volume. This was expected, given the abundant expression of u-PAR in all tumors. u-PAR expression was also independent of the clinical response to platinum-based chemotherapy ("platinum sensitivity") and the amount of residual tumor at the end of surgery. Expression of u-PAR was low to absent in normal surface epithelium of the ovary and fallopian tube (Fig. 1A). To determine if expression of u-PAR is a prognostic factor in ovarian cancer, a Kaplan–Meier analysis was performed. The median overall survival in women with high (score $\geq$ 120) u-PAR expression was 33 months and 45 months in women with low (score < 120) u-PAR expression ($P = 0.15$; Fig. 1B), a difference that did not reach statistical significance. Furthermore, there was no statistical difference in progression free survival (PFS) of women with low levels of u-PAR (median PFS 16.1 months) when compared with women with high levels (median PFS 13.1 months). There was also no difference in the level of u-PAR expression in early and late tumor stages or between the primary ovarian tumor and the corresponding omental (n = 61) or peritoneal metastases (n = 50; Fig. 1C). Taken together, these data indicate that, while u-PAR expression was not shown to be a prognostic factor, u-PAR is expressed in the majority of ovarian tumors, both primary and metastatic, and, therefore, could prove to be a valuable target for the treatment of ovarian cancer.

u-PAR contributes to ovarian cancer cell adhesion, migration, and invasion

Given the expression of u-PAR in the majority of ovarian cancers, several ovarian cancer cell lines were characterized for their u-PAR expression. All cell lines, including the primary ovarian cancer cell line MONTY-1 (11), expressed at least a low level of u-PAR. CaOV3 (high-), HeyA8 (moderate-), or SKOV3ip1 (low-u-PAR expression) were chosen for the subsequent experiments (Fig. 2A). Ovarian cancer metastasis involves the adhesion, migration, and invasion of tumor cells to the peritoneal cavity. To determine if u-PAR is involved in these processes, cells were treated with a u-PAR antibody (ATN-658) that inhibits the downstream signaling of u-PAR (10). Simultaneous treatment of cells with the u-PAR antibody at the time of the assay had no effect on adhesion, whereas the pretreatment of cells for 18 hours resulted in a modest inhibition of ovarian cancer cell adhesion (Fig. 2B). Dissociation of endogenous uPA and u-PAR with a mild acid wash had no effect on ovarian cancer cell adhesion (Supplementary

Published OnlineFirst December 13, 2010; DOI: 10.1158/1078-0432.CCR-10-2258

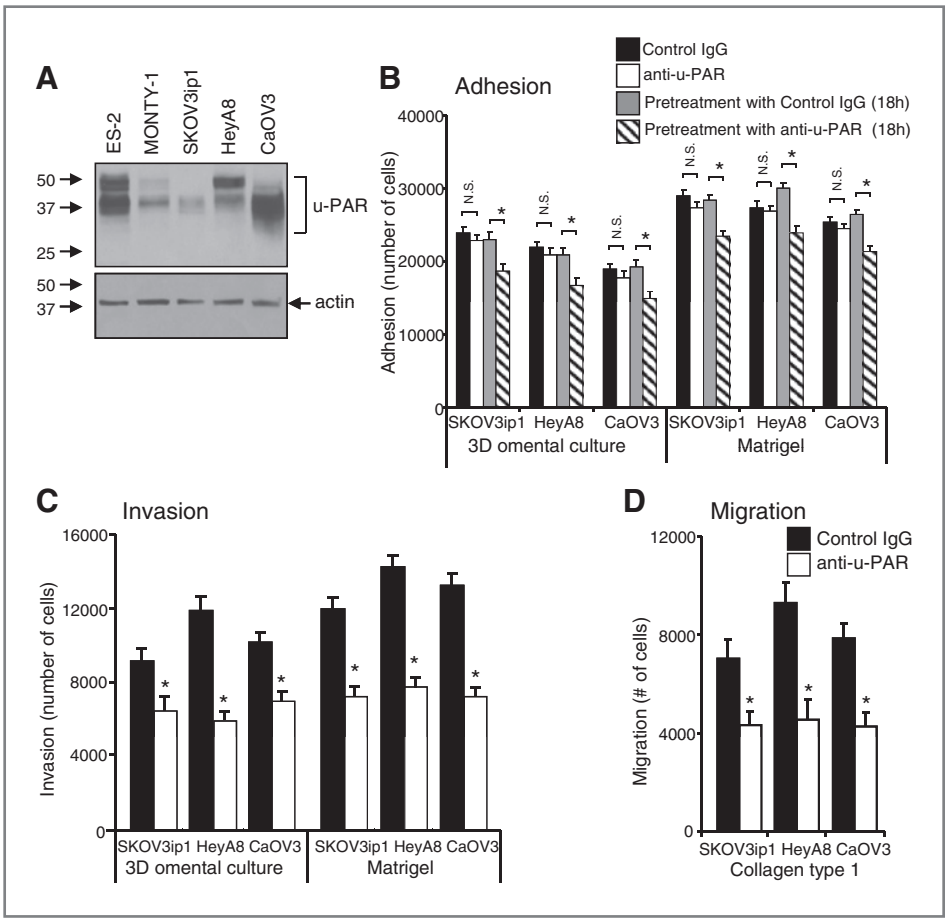

Figure 2. Anti-u-PAR treatment of ovarian cancer cells reduces cell adhesion, migration, and invasion *in vitro*. A, immunoblot analysis of u-PAR levels in ovarian cancer cells, including the primary ovarian cancer cell line, MONTY-1. B, effect of u-PAR antibody treatment on adhesion after 30 minutes to the 3D omental culture or Matrigel, with anti-u-PAR added at time of the assay or 18 hours prior to assay. C, effect of u-PAR antibody treatment on ovarian cancer cell invasion into the 3D omental culture or Matrigel after 24 hours. D, effect of u-PAR antibody treatment on ovarian cancer cell migration through collagen type 1 after 24 hours. Mouse IgG was added as the negative control. Each bar is the mean +/- standard deviation of $n = 5$ (B–D), and is representative of 3 independent experiments. A Student's t test compares the 2 treatments noted with brackets. *, $P < 0.01$ between control IgG and experimental treatment; N.S., not significant.

Fig. S1). In contrast, the u-PAR antibody significantly inhibited ovarian cancer cell invasion through Matrigel, and through a 3D omental culture that mimics the microenvironment of ovarian cancer cells (ref. 13; Fig. 2C), as well as migration through type I collagen (Fig. 2D). Anti-u-PAR treatment had no effect on ovarian cancer cell proliferation (Supplementary Fig. S2).

Blocking u-PAR inhibits orthotopic ovarian cancer growth in mice

To evaluate the effect of the u-PAR antibody *in vivo*, we used the same ovarian cancer cell lines in an orthotopic ovarian cancer xenograft model. Cells were injected i.p., and 7 days later, ATN-658 or mouse IgG (control) administered alone or in combination with paclitaxel, a drug currently used as a front-line treatment in patients with ovarian cancer. In the SKOV3ip1 and CaOV3 tumor-bearing mice, anti-u-PAR treatment resulted in a statistically significant reduction in mean tumor weight ($P < 0.01$) and number of metastasis ($P < 0.01$) compared with the control IgG-treated mice (Fig. 3A). Paclitaxel treatment decreased mean tumor weight and the number of tumors ($P < 0.01$). The combination of anti-u-PAR and paclitaxel treatment had a greater effect on the reduction of tumor weight ($P < 0.01$) than either treatment alone in the SKOV3ip1 xenograft model, as well as on the reduction of tumor weight ($P < 0.05$) and number ($P < 0.01$) in the CaOV3 xenograft model. In the HeyA8tumor-bearing mice, which only produce a few solid tumors, anti-u-PAR treatment resulted in a decrease in tumor weight ($P < 0.01$) compared with IgG control (Fig. 3B). Again, paclitaxel treatment resulted in a greater reduction of tumor weight, which also increased when combined with the u-PAR antibody ($P < 0.05$). To determine if anti-u-PAR treatment significantly changed survival in an OvCa xenograft model, Kaplan–Meier analysis of a survival study with the HeyA8 xenograft model was performed. Treatment with the u-PAR antibody led to increased survival in the HeyA8 xenograft model (Fig. 3B) compared with IgG-treated mice ($P < 0.0001$). Paclitaxel increased overall survival rate regardless of antibody treatment ($P < 0.0001$), and a further increase in survival rate was observed in mice treated with anti-u-PAR in combination with paclitaxel ($P = 0.002$).

u-PAR antibody treatment inhibits u-PAR and uPA expression

Next, we evaluated the effect of u-PAR antibody treatment on u-PAR and uPA expression *in vivo* and *in vitro*.

Published OnlineFirst December 13, 2010; DOI: 10.1158/1078-0432.CCR-10-2258

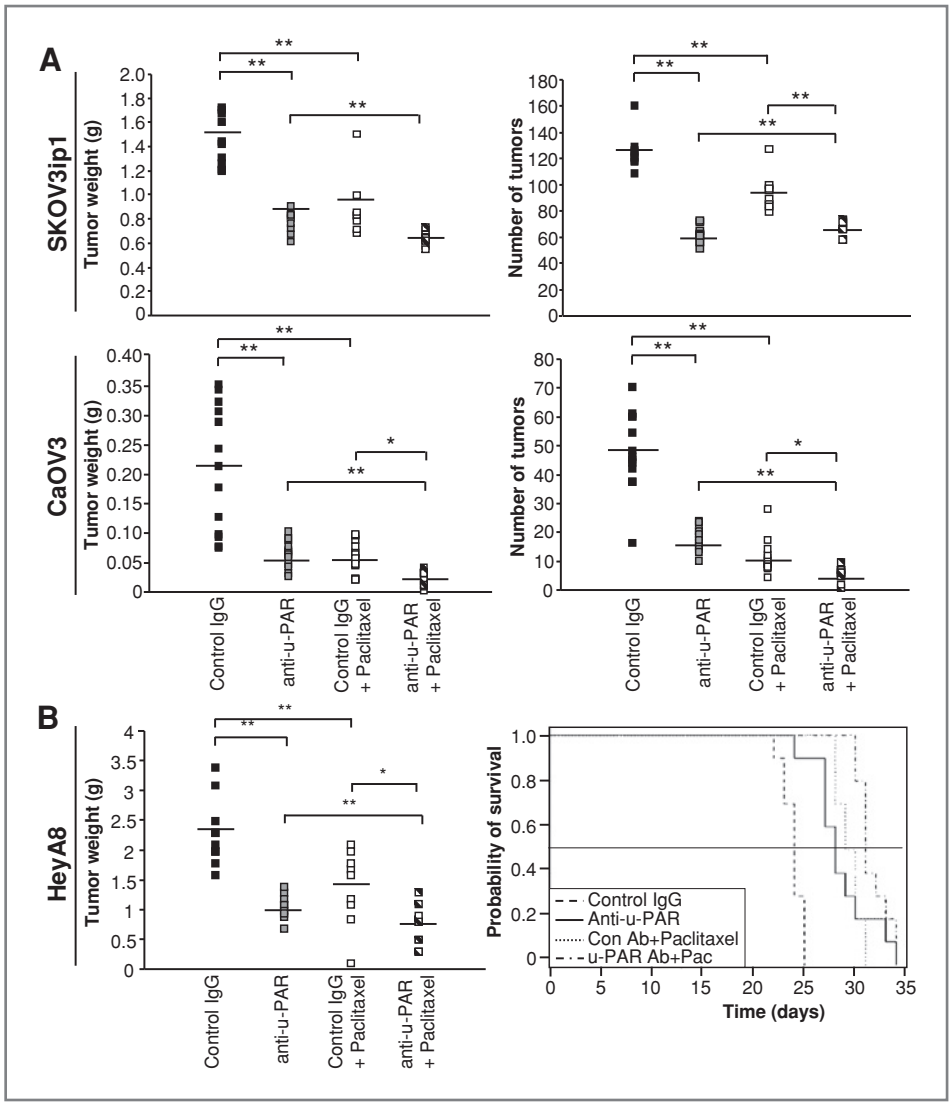

Figure 3. Treatment with an u-PAR antibody significantly reduces tumor weight. A, tumor weight and number in SKOV3ip1 (10 mice/treatment) and CaOV3 (13 mice/treatment) ovarian cancer cell xenograft models treated with control IgG, u-PAR antibody (10 mg/kg) and/or paclitaxel (1.5 mg/kg). B, tumor weight and survival of HeyA8 (10 mice/treatment) ovarian cancer cell xenograft models treated with control IgG, u-PAR antibody (10 mg/kg) and/or paclitaxel (1.5 mg/kg). For tumor weight, the mean (bar) and each animal (square) are presented (A and B). A Student's *t* test compares the 2 treatments noted with brackets; *, $P < 0.05$ and **, $P < 0.01$ between control IgG and experimental treatment. For survival (B), the Kaplan–Meier survival curve is presented (*P*-values from log rank test results are presented in Results section).

Tumors from anti-u-PAR-treated mice had lower u-PAR and uPA mRNA and protein expression levels compared with tumors from mice treated with IgG (Fig. 4A). *In vitro*, fluorescently labeled OvCa cells were cultured on plastic or added to the 3D omental culture, which was composed of a single layer of mesothelial cells overlaying fibroblasts plated in collagen ECM. Fluorescently activated cell sorting was used to sort the OvCa cells from the 3D culture, and mRNA and protein expression levels were tested. The u-PAR mRNA and protein expression in all 3 tumor cell lines increased significantly upon coculture with the 3D omental culture, suggesting that the interaction of cancer cells with mesothelial cells and fibroblasts induces u-PAR expression. These effects could be inhibited by at least 60% with u-PAR antibody treatment (Fig. 4B). Although uPA mRNA and protein levels were not further induced by the 3D culture compared with plastic, its constitutive expression in the tumor cells was still blocked by the u-PAR antibody.

The effect of anti-u-PAR treatment on the localization of u-PAR in cancer cells cultured on omental ECM was investigated. We believed that ECM isolated from benign human omentum would provide a microenvironment that was more comparable to the human omentum, the most common site of OvCa metastasis, than Matrigel or collagen alone. u-PAR was localized on tumor cells using FITC-labeled uPA (Fig. 4C). Once again, anti-u-PAR treatment inhibited the constitutive u-PAR expression of cells cultured on plastic or omental ECM. Moreover, when cancer cells were treated with control IgG, u-PAR localized at the site of contact with primary human omental ECM (top square panels; bottom rectangular panels, 0 μm). However, after anti-u-PAR treatment, u-PAR did not cluster in this fashion but was more uniformly distributed in the cells.

Published OnlineFirst December 13, 2010; DOI: 10.1158/1078-0432.CCR-10-2258

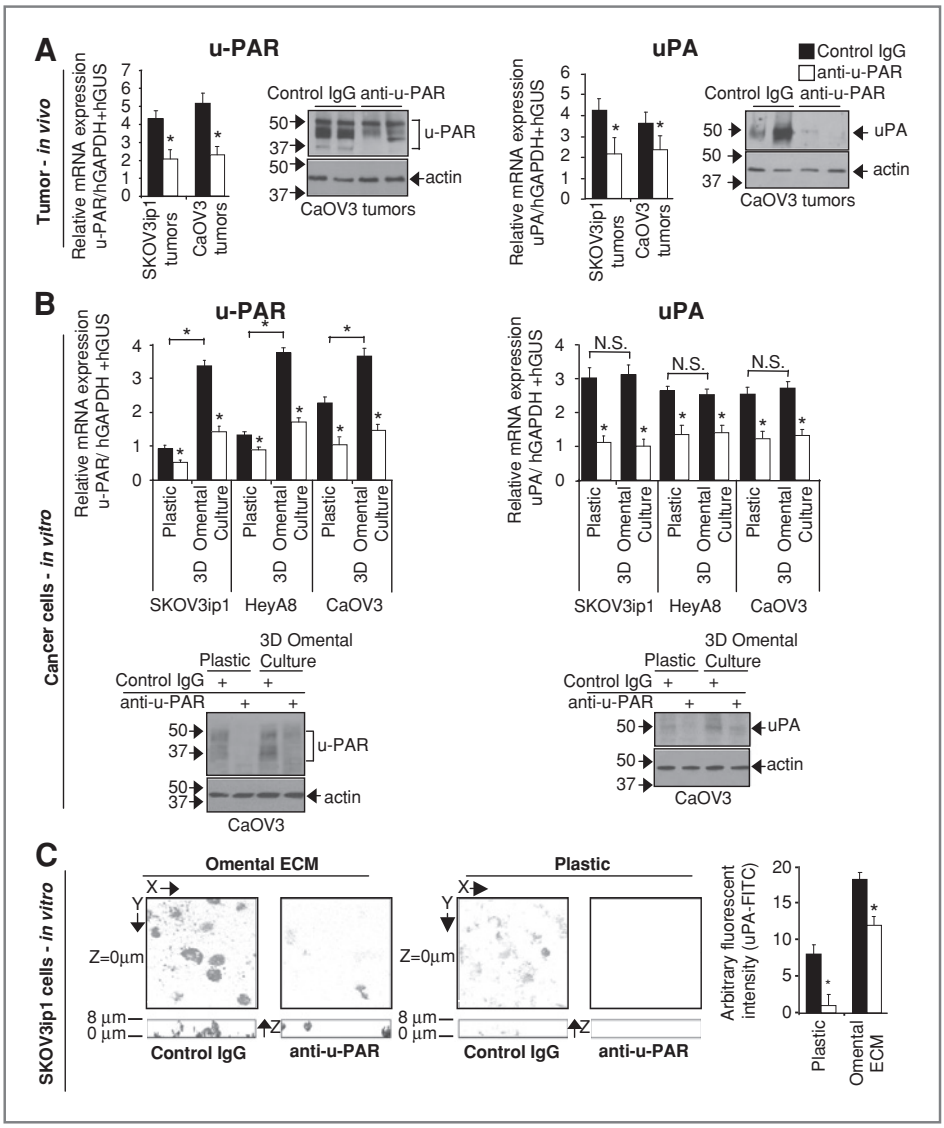

Figure 4. Anti-u-PAR treatment decreases u-PAR and uPA expression *in vivo* and *in vitro*. A and B, the effect of anti-u-PAR treatment on u-PAR and uPA was tested *in vivo* in the SKOV3ip1 and CaOV3 xenograft models and *in vitro* in SKOV3ip1, HeyA8, and CaOV3 cells grown on plastic or the 3D omental culture. Anti-u-PAR treatment significantly reduced u-PAR and uPA mRNA (qRT-PCR) and protein (immunoblot) levels in xenograft ovarian cancer tumors (A) and in ovarian cancer cells (B) cultured on plastic or the 3D culture. Bar graph show results representative of 3 independent experiments and shows results of ($n = 5$, *in vitro*; $n = 3$, *in vivo*) +/- standard deviation. C, Tumor cell/Omental ECM interaction. 3D localization of FITC-labeled uPA (signal in gray) in SKOV3ip1 cells cultured on plastic or omental ECM (630× magnification). The XY images (square/top images) are taken at Z-plane (depth) of contact ($Z = 0$ μm) between ovarian cancer cell and plastic/omental ECM, and the Z image (rectangle/bottom) is a cumulative image (Z-stack) of cells on plastic/omental ECM. The level of FITC-uPA in SKOV3ip1 cells on plastic or omental ECM with control IgG or anti-u-PAR treatment was measured by a fluorescent-plate reader, and reported as arbitrary fluorescent units. Each bar is the mean +/- standard deviation of $n = 5$, and is representative of 5 independent experiments. A Student's *t* test compares control to u-PAR antibody treatment in each graph (A–C) and the 2 treatments noted with brackets. *, $P < 0.05$; N.S., not significant.

Blocking u-PAR affects integrin signaling and induces apoptosis

We then took an unbiased approach to investigate mRNA changes affected by u-PAR antibody treatment *in vivo*. Microarray analysis was performed on RNA isolated from mouse ovarian cancer cell xenograft tumors excised after 4 doses of u-PAR antibody or control IgG. Gene expression analysis revealed that the pathway most significantly regulated by ATN-658 treatment involved integrin signaling. The gene expression profile of integrin signaling in tumors from CaOV3 xenograft mice treated with anti-u-PAR compared with control IgG is shown in Figure 5A. We confirmed and tested 10 of the regulated genes, including ACTG2, the mRNA with greatest fold difference between treated and untreated mice. u-PAR antibody treatment decreased

Published OnlineFirst December 13, 2010; DOI: 10.1158/1078-0432.CCR-10-2258

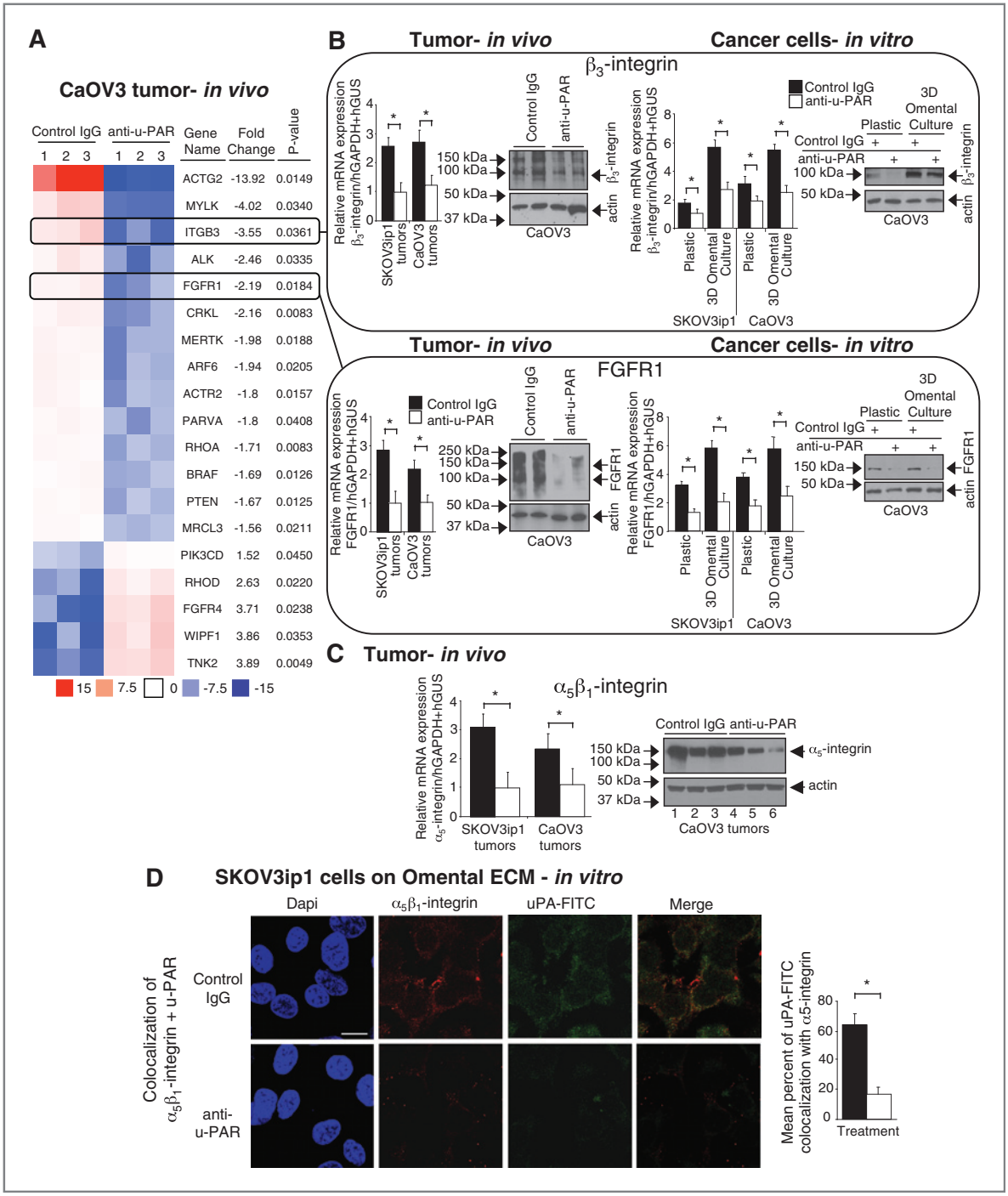

Figure 5. Anti-u-PAR treatment decreases integrin signaling. A, gene array analysis of expression changes of mRNAs involved in integrin signaling. Shown is relative fold-difference in the 19 genes, which were significantly regulated at least 1.5-fold in anti-u-PAR compared with control IgG treatment. B, the effect of anti-u-PAR treatment on β_3-integrin and FGFR1 was tested *in vivo* in the SKOV3ip1 and CaOV3 xenograft models and *in vitro* in SKOV3ip1 and CaOV3 cells grown on plastic or the 3D omental culture. Anti-u-PAR treatment significantly reduced β_3-integrin and FGFR1 mRNA (qRT-PCR) and protein (immunoblot) levels in xenograft ovarian cancer tumors and in ovarian cancer cells cultured on plastic or the 3D culture. Bar graph shows results from 3 independent experiments ($n = 5$, *in vitro,* B) and 3 animals (*in vivo,* B) +/- standard deviation. C, the effect of anti-u-PAR treatment on α_5-integrin expression was determined *in vivo*. Anti-u-PAR treatment significantly reduced α_5-integrin RNA (qRT-PCR) and protein (immunoblot) levels in xenograft ovarian cancer tumors. Bar graph shows results from 3 animals (*in vivo,* C) +/- standard deviation. D, colocalization of u-PAR and α_5-integrin on omental ECM in ovarian cancer cells. SKOV3ip1 cells cultured on omental ECM were stained with FITC-labeled uPA and immunofluorescence for α_5-integrin was performed. Bar graph shows mean percent of uPA-FITC colocalization with α_5-integrin as calculated using the Imaris colocalization application (details in the Materials and Methods section). Bar graphs show mean +/- standard deviation ($n = 5$, *in vitro*) and are representative of 3 independent experiments. A Student's *t* test compares the 2 treatments noted with brackets. *, $P < 0.01$.

Published OnlineFirst December 13, 2010; DOI: 10.1158/1078-0432.CCR-10-2258

ACTG2 protein and mRNA expressoin *in vivo* and *in vitro* (Supplementary Fig. S3).

In view of the inhibitory effect of u-PAR antibody treatment on ovarian cancer cell adhesion, migration, and invasion, we were particularly interested in confirming the downregulation of 2 genes with known involvement in these processes, β_3-integrin and FGFR1 (11, 25). Treatment with the u-PAR antibody inhibited β_3-integrin and FGFR1 mRNA and protein expression *in vivo*. This was confirmed *in vitro* in 2 cell lines (SKOV3ip1 and CaOV3). Treatment of cells on plastic, as well as on the 3D culture, resulted in an inhibition of β_3-integrin and FGFR1 mRNA and protein expression (Fig. 5B).

Previous studies have shown that the association of u-PAR with the fibronectin receptor ($\alpha_5\beta_1$-integrin) affects the expression and activation state of u-PAR and that u-PAR is important for tumor cell invasion (26, 27). Therefore, we determined if the antibody affects the expression of α_5-integrin and the interaction of u-PAR and α_5-integrin. Indeed, treatment with the u-PAR antibody in the CaOV3 xenograft model inhibited α_5-integrin mRNA and protein expression (Fig. 5C). *In vitro*, the anti-u-PAR treatment inhibited colocalization of α_5-integrin and u-PAR in SKOV3ip1 cells cultured on primary human omental ECM (Fig. 5D). For the colocalization experiments, the live cells were incubated with FITC-labeled uPA, just prior to fixation (28). Subsequently, immunofluorescence with an α_5-integrin specific antibody, confocal microscopy, and image analysis were performed.

The histologic appearance of u-PAR and IgG-treated tumors was very similar and there was no difference between angiogenesis (microvessel density) and proliferation (Ki-67) in tumors from u-PAR antibody or mouse IgG antibody-treated mice (Fig. 6). However, anti-u-PAR treatment increased cleaved-caspase 3 expression and DNA fragmentation of ovarian tumor cells in CaOV3 and SKOV3ip1 xenografts (TUNEL staining; Fig. 6A). The effect of anti-u-PAR treatment on apoptosis was confirmed *in vitro* (Fig. 6B). Treatment with the u-PAR antibody increased expression of active caspase 3 in SKOV3ip1 and CaOV3 cells, DNA fragmentation of SKOV3ip1 cells, and the percent of apoptotic cells in SKOV3ip1 cells when compared with control antibody treated cells (Fig. 6B).

Discussion

Since the discovery of the u-PAR in 1985 (29, 30), 25 years of intensive research has elucidated its role as a multifunctional receptor involved in a myriad of tumor cell processes, including invasion, ECM remodeling, adhesion, migration, angiogenesis, and metastasis (4–6). However, although u-PAR's many roles in cancer makes it a very attractive therapeutic target, its potential has yet to be translated into a clinical benefit. As a first step toward defining u-PAR's potential in ovarian cancer treatment, we characterized its expression level and found that over 90% of all epithelial ovarian cancers expressed u-PAR protein in the epithelial tumor compartment. u-PAR was expressed in both the primary tumor and the metastases and in early and as well as late tumor stages, suggesting that it is upregulated in early ovarian tumorigenesis. These results corroborate previously published studies on u-PAR expression in primary ovarian tumors. In a review of all published studies reporting u-PAR expression, we found 7 studies that reported that greater than 80% of all ovarian cancer tumors express the u-PAR (summarized in Supplementary Table S1) and 2 studies that reported lower levels of u-PAR in ovarian cancer (22, 23). These expression studies and the well-established importance of u-PAR in cancer biology suggest that all patients with the u-PAR-expressing tumors could potentially benefit from u-PAR-targeted therapy and support our proposal to test u-PAR inhibition as an anticancer strategy.

The efficacy of the u-PAR antibody in the inhibition of various ovarian cancer cell functions was explored both *in vitro* and *in vivo*. We tested the effects of this antibody in 3 different ovarian cancer cell lines to increase the likelihood of generalizable results (31, 32). Our results overwhelmingly show that the u-PAR antibody is able to inhibit the adhesion, migration, and invasion of all tested ovarian cancer cell lines *in vitro* and in a 3D model, as well as to inhibit metastasis in 3 different ovarian xenograft models. These results are in agreement with those of other investigators who have identified u-PAR as a therapeutic target in preclinical models of cancer. Two studies by the same group specifically investigated the targeting of u-PAR in ovarian cancer. First, Sato and colleagues, using the OVMZ-6 ovarian cancer xenograft mouse model, identified 2 cyclic peptides which act as competitive antagonists of the uPA/u-PAR interaction and were able to reduce tumor weight *in vivo* (33). Second, Knör and colleagues successfully targeted u-PAR in OVMZ-6 ovarian cancer cells in culture, which inhibited colony formation (34). The urokinase receptor has also been successfully inhibited using various techniques in other cancers, including DNAzymes (osteosarcoma) (35), siRNA (glioma) (9), monoclonal antibodies (pancreatic, colorectal, and prostate) (10, 28, 36), and u-PAR antagonists (melanoma and colorectal cancer) (37, 38). Although most of these studies successfully targeted u-PAR in preclinical models of cancer and resulted in various degrees of disruption of known u-PAR functions, most of the reported methods used to inhibit u-PAR are not ready for further clinical development because of short half-life of the agents and concerns involving their purity, stable delivery, and safety. Monoclonal antibodies, however, have finally come of age as therapeutics, and several molecules have recently been approved as cancer therapies. Therefore, given the encouraging results in this and other preclinical studies (10, 36), we believe that an

Published OnlineFirst December 13, 2010; DOI: 10.1158/1078-0432.CCR-10-2258

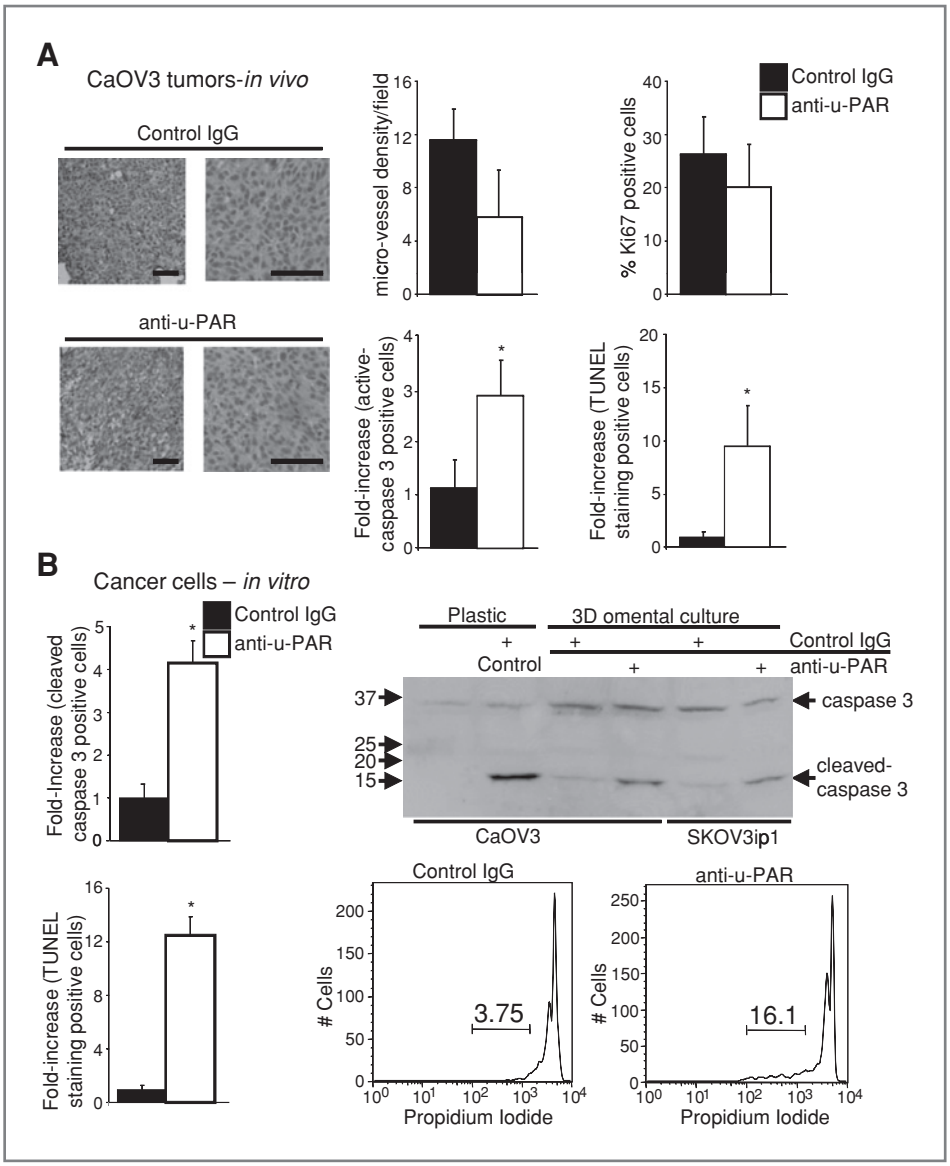

Figure 6. Treatment with an u-PAR antibody increases apoptosis of ovarian cancer cells. A, effects of u-PAR antibody treatment *in vivo*. Representative images of tumors stained with hematoxylin and eosin are shown (100× and 200× magnification). Analysis of microvessel density (CD31), proliferation (Ki-67), and apoptosis (activated caspase 3 and TUNEL staining), by immunohistochemistry of CaOV3 xenograft tumor cross-sections. B, effects of anti-u-PAR treatment for 48 hours in ovarian cancer cells cultured on plastic or 3D omental culture *in vitro*. Analysis of apoptosis by immunofluorescence and immunoblot for cleaved caspase 3, TUNEL staining, or propidium iodide staining with FACS (percent of sub-G_1 fraction is indicated). Bar graph shows results of 3 animals (*in vivo,* A) +/- standard deviation and results ($n = 5$, *in vitro,* B) representative of 3 independent experiments. A Student's *t* test compares control to u-PAR antibody treatment in each graph. *, $P < 0.01$. For immunoblot of caspase 3, CaOV3 cells on plastic were treated with staurosporine for 3 hours and protein lysates collected (positive control).

antibody against u-PAR has the potential to be advanced into clinical testing.

In view of previous observations that u-PAR directly binds to adhesion molecules, we investigated whether anti-u-PAR treatment affects u-PAR interaction with integrins. We found that the u-PAR antibody inhibited the association of u-PAR with $\alpha_5\beta_1$-integrin. This finding is in agreement with results of the study by Wei and colleagues, which determined that u-PAR directly binds and activates $\alpha_5\beta_1$-integrin, causing a conformational change in $\alpha_5\beta_1$-integrin that permits binding to a different fragment of fibronectin and increased invasion (27). In addition, β_3-integrin was consistently downregulated by anti-u-PAR treatment. In glioma cells, adenovirus-mediated downregulation of u-PAR was also found to inhibit $\alpha_v\beta_3$-integrin expression (39). Therefore, it is apparent that u-PAR inhibition modifies both the interaction and expression of integrins, suggesting that u-PAR can differentially affect integrin functions. In addition, anti-u-PAR treatment increased cleaved-caspase 3 expression, the percentage of apoptotic cells, and DNA fragmentation, explaining further why the treated tumors are smaller. Gondi and colleagues (40) also reported that u-PAR and uPA inhibition induces caspase-mediated apoptosis. Conversely, these results also suggest that u-PAR supports aberrant cell survival in tumor cells.

In summary, we show that u-PAR is widely expressed in ovarian carcinomas and that treatment with an u-PAR antibody targeted and inhibited u-PAR-dependent functions, including ovarian cancer cell invasion and metastasis. In view of the encouraging preclinical results shown in this and other studies targeting u-PAR, we propose that sufficient rationale exists to evaluate the effects of u-PAR inhibition in clinical cancer trials.

Published OnlineFirst December 13, 2010; DOI: 10.1158/1078-0432.CCR-10-2258

Disclosure of Potential Conflicts of Interest

The ATN-658 u-PAR antibody was supplied by Attenuon, which also provided funding for the animal experiments. A. Mazar was a former employee of Attenuon who developed the u-PAR antibody and has a patent application submitted on the antibody.

Acknowledgments

We thank Dr. Hal Chapman (University of California, San Francisco, Pulmonary and Critical Care Division) for his kind advice, Dr. Karl Matlin (University of Chicago, Department of Surgery) for use of the confocal microscope, and Gail Isenberg for editorial assistance.

Grant Support

H.A. Kenny is supported by the National Cancer Institute (K99CA134750). E. Lengyel holds a Clinical Scientist Award in Translational Research from the Burroughs Wellcome Fund, and is supported by grants from the Ovarian Cancer Research Fund (Liz Tilberis Scholars Program), and the National Cancer Institute (R01CA111882).

The costs of publication of this article were defrayed in part by the payment of page charges. This article must therefore be hereby marked *advertisement* in accordance with 18 U.S.C. Section 1734 solely to indicate this fact.

Received August 23, 2010; revised November 17, 2010; accepted November 30, 2010; published OnlineFirst December 13, 2010.

References

1. Cannistra SA. Cancer of the ovary. N Engl J Med 2004;351:2519–29.
2. Bast RC, Hennessy B, Mills GB. The biology of ovarian cancer: new opportunities for translation. Nat Rev Cancer 2009;9:415–28.
3. Lengyel E. Ovarian cancer development and metastasis. Am J Pathol 2010;177:1053–64.
4. Blasi F, Carmeliet P. uPAR: a versatile signalling orchestrator. Nat Rev Mol Cell Biol 2002;3:932–43.
5. Mazar AP. Urokinase plasminogen activator receptor choreographs multiple ligand interactions: implications for tumor progression and therapy. Clin Cancer Res 2008;14:5649–55.
6. Smith HW, Marshall CJ. Regulation of cell signalling by uPAR. Nat Rev Mol Cell Biol 2010;11:23–36.
7. Dass K, Ahmad A, Azmi AS, Sarkar S, Sarkar FH. Evolving role of uPA/uPAR system in human cancers. Cancer Treat Rev 2008; 34:122–36.
8. Kook YH, Adamski J, Zelent A, Ossowski L. The effect of antisense inhibition of urokinase receptor in human squamous cell carcinoma on malignancy. EMBO J 1994;13:3983–91.
9. Gondi CS, Lakka SS, Dinh DH, Olivero WC, Gujrati M, Rao JS. RNAi-mediated inhibition of cathepsin B and uPAR leads to decreased cell invasion, angiogenesis and tumor growth in gliomas. Oncogene 2004;23:8486–96.
10. Bauer TW, Liu W, Fan F, Camp ER, Yang A, Somcio RJ, et al. Targeting of urokinase plasminogen activator receptor in human pancreatic carcinoma cells inhibits c-met and insulin-like growth factor-1 receptor-mediated migration and invasion and orthotopic tumor grwoth in mice. Cancer Res 2005;17:7775–81.
11. Kaur S, Kenny HA, Jagadeeswaran S, Zillhardt MR, Montag AG, Kistner E, et al. β3 -integrin expression on tumor cells inhibits tumor progression, reduces metastasis, and is associated with a favorable prognosis in patients with ovarian cancer. Am J Pathol 2009; 175:2184–96.
12. Sawada K, Radjabi AR, Shinomiya N, Kistner E, Kenny H, Becker AR, et al. c-Met overexpression is a prognostic factor in ovarian cancer and an effective target for inhibition of peritoneal dissemination and invasion. Cancer Res 2007; 67:1670–80.
13. Kenny HA, Krausz T, Yamada SD, Lengyel E. Use of a novel 3D culture model to elucidate the role of mesothelial cells, fibroblasts and extracellular matrices on adhesion and invasion of ovarian cancer cells. Int J Cancer 2007;121:1463–72.
14. Kenny HA, Kaur S, Coussens L, Lengyel E. The initial steps of ovarian cancer cell metastasis are mediated by MMP-2 cleavage of vitronectin and fibronectin. J Clin Invest 2008;118:1367–79.
15. Abberton KM, Bortolotto SK, Woods AA, Findlay M, Morrison WA, Thompson EW, et al. Myogel, a novel, basement membrane-rich, extracellular matrix derived from skeletal muscle, is highly adipogenic in vivo and in vitro. Cells Tissues Organs 2008;188:347–58.
16. Pfaffl M. A new mathematical model for relative quantification in real-time RT-PCR. Nucleic Acids Res 2001;29:2002–7.
17. Casslen B, Gustavsson B, Astedt B. Cell membrane receptors for urokinase plasminogen activator are increased in malignant ovarian tumors. Eur J Cancer 1991;27:1445–8.
18. Borgfeldt C, Bendahl PO, Gustavsson B, Långström E, Fernö M, Willén R, et al. High tumor tissue concentration of urokinase plasminogen activator receptor is associated with good prognosis in patients with ovarian cancer. Int J Cancer 2003;107:658–65.
19. Borgfeldt C, Hansson S, Gustavsson B, Måsbäck A, Casslen B. Dedifferentiation of serous ovarian cancer from cystic to solid tumors is associated with increased expression of mRNA for urokinase plasminogen activator (uPA), its receptor (uPAR) and its inhibitor PAI-1. Int J Cancer 2001;92:497–502.
20. Tecimer C, Doering DL, Goldsmith LJ, Meyer JS, Abdulhay G, Wittliff JL. Clinical relevance of urokinase-type plasminogen activator, its receptor and inhibitor type 1 in ovarian cancer. Int J Gynecol Cancer 2000;10:372–81.
21. Schmalfeldt B, Kuhn W, Reuning U, Pache L, Dettmar P, Schmitt M, et al. Primary tumor and metastasis in ovarian cancer differ in their content of urokinase-type plasminogen activator, its receptor, and inhibitors types 1 and 2. Cancer Res 1995;55:3958–63.
22. Mabrouk R, Ali-Labib R. Detection of urokinase plasminogen activator receptor and c-erbB-2 in sera of patients with breast and ovarian carcinoma. Clin Biochem 2003;36:537–43.
23. Chambers SK, Ivins CM, Carcangiu ML. Urokinase-type plasminogen activator in epithelial ovarian cancer: a poor prognostic factor, associated with advanced stage. Int J Gynecol Cancer 1998;8:242–50.
24. Wang L, Madigan MC, Chen H, Liu F, Patterson KI, Beretov J, et al. Expression of urokinase plasminogen activator and its receptor in advanced epithelial ovarian cancer patients. Gynecol Oncol 2009;114:265–72.
25. Suyama K, Shapiro I, Guttman M, Hazan RB. A signaling pathway leading to metastasis is controlled by N-cadherin and the FGF receptor. Cancer Cell 2010;2:301–14.
26. Tarui T, Andronicos N, Czekay RP, Mazar AP, Bdeir K, Parry GC, et al. Critical role of integrin α5β1 in urokinase (uPA)/urokinase receptor (uPAR, CD87) signaling. J Biol Chem 2003;278:29863–72.
27. Wei Y, Tang C, Kim Y, Robillard L, Zhang F, Kugler MC, et al. Urokinase receptors are required for α5β1 integrin-mediated signaling in tumor cells. J Biol Chem 2007;282: 3929–39.
28. Rabbani SA, Ateeq B, Arakelian A, Valentino ML, Shaw DE, Dauffenbach LM, et al. An anti-urokinase plasminogen activator antibody (ATN-658) blocks prostate cancer invasion, migration, growth, and experimental skeletal metastasis in vitro and in vivo. Neoplasia 2010;12:778–88.
29. Stoppelli MP, Corti A, Soffientini A, Cassanni G, Blasi F, Assoian R. Differentiation-enhanced binding of the amino-terminal fragment of human urokinase plasminogen activator to a specific receptor on U937 monocytes. Proc Natl Acad Sci U S A 1985;82:4939–43.
30. Vassalli JD, Baccino D, Belin D. A cellular binding site for the Mr 55,000 form of the human plasminogen activator, urokinase. J Cell Biol 1985;100:86–92.
31. Frederick PJ, Straughn JM, Alvarez RD, Buchsbaum HJ. Preclinical studies and clinical utilization of monoclonal antibodies in epithelial ovarian cancer. Gynecol Oncol 2009;113:384–90.
32. Voskoglou-Nomikos T, Pater JL, Seymour L. Clinical predicitive value of the in vitro cell line, human xenograft, and mouse allograft preclinical cancer models. Clin Cancer Res 2003;9:4227–39.

Published OnlineFirst December 13, 2010; DOI: 10.1158/1078-0432.CCR-10-2258

33. Sato S, Kopitz C, Schmalix WF, Muehlenweg B, Kessler H, Schmitt M, et al. High-affinity urokinase-derived cyclic peptides inhibiting urokinase/urokinase receptor-interaction: effects on tumor growth and spread. FEBS Lett 2002;528:212–6.
34. Knör S, Sato S, Huber T, Morgenstern A, Bruchertseifer F, Schmitt M, et al. Development and evaluation of peptidic ligands, targeting tumour-associated urokinase plasminogen activator receptor (uPAR) for use in alpha-emitter therapy for disseminated ovarian cancer. Eur J in Nucl Med Mol Imaging 2008;35:53–64.
35. de Bock CE, Lin Z, Itoh T, Morris D, Murrell G, Wang Y. Inhibition of urokinase receptor gene expression and cell invasion by anti-uPAR DNAzymes in osteosarcoma cells. FEBS J 2005;272:3572–82.
36. Van Buren G 2nd, Gray MJ, Dallas NA, Xia L, Lim SJ, Fan F, et al. Targeting the urokinase plasminogen activator receptor with a monoclonal antibody impairs the growth of human colorectal cancer in the liver. Cancer 2009;115:3360–8.
37. Min HY, Doyle LV, Vitt CR, Zandonella CL, Stratton-Thomas JR, Shuman MA, et al. Urokinase receptor antagonists inhibit angiogenesis and primary tumor growth in syngeneic mice. Cancer Res 1996;56:2428–33.
38. Ignar DM, Andrews JL, Witherspoon SM, Leray JD, Clay WC, Kilpatrick K, et al. Inhibition of establishment of primary and micrometastatic tumors by a urokinase plasminogen activator receptor antagonist. Clin Exp Metastasis 1998;16:9–20.
39. Lutz V, Reuning U, Krüger A, Luther T, von Steinburg SP, Graeff H, et al. High level synthesis of recombinant soluble urokinase receptor (CD87) by ovarian cancer cells reduces intraperitoneal tumor growth and spread in nude mice. Biol Chem 2001;382:789–98.
40. Gondi CS, Kandhukuri N, Dinh DH, Gujrati M, Rao JS. Downregulation of uPAR and uPA activates caspase mediated apoptosis, inhibits the PI3kinase/AKT pathway. Int J Oncol 2007;31:19–27.

AACR American Association for Cancer Research

Clinical Cancer Research

Targeting the Urokinase Plasminogen Activator Receptor Inhibits Ovarian Cancer Metastasis

Hilary A. Kenny, Payton Leonhardt, Andras Ladanyi, et al.

Clin Cancer Res 2011;17:459-471. Published OnlineFirst December 13, 2010.